The molecular mechanism of Radix astragali, Ginseng, Radix puerariae, and Mulberry leaf in the treatment of diabetic cardiomyopathy based on bioinformatics and network pharmacology

Xingchen Guo
Department of Cardiology, People's Hospital of Zhengzhou University, Zhengzhou University
Wanhao Gao
Department of Cardiology, People's Hospital of Zhengzhou University, Zhengzhou University
Dongdong Zhang (sedate@stu.shzu.edu.cn)
School of life sciences, Shihezi University
Muwei Li
Department of Cardiology, People's Hospital of Zhengzhou University, Zhengzhou University

Research Article

Keywords: Molecular dynamics simulation, PI3K-Akt signaling pathway, mTOR signaling pathway, Diabetic cardiomyopathy, Puerarin

Posted Date: April 13th, 2022

DOI: https://doi.org/10.21203/rs.3.rs-1507973/v2

Abstract

Objective

To evaluate the therapeutic effects of traditional Chinese medicines Radix astragali (Huangqi, HQ), Ginseng (Renshen, RS), Radix puerariae (Gegen, GG), and Mulberry leaf (Sangye, SY) on diabetic cardiomyopathy (DC) based on bioinformatics and network pharmacology, through gene expression analysis of geo clinical samples, molecular docking of compounds and targets, and molecular dynamics simulation, and to discover new targets for prevention or treatment of DC, in order to facilitate and better serve the discovery of new drugs as well as their application in the clinic.

Materials and methods

For the initial selection of ingredients and targets using the TCMSP as a starting point, we performed a primary screening of ingredients and targets of the four herbs using tools including Cytoscape, Tbtools, R 4.0.2, Autodock Vina, PyMOL, and GROMACS. To further screen the effective ingredients and targets, we performed protein interaction network (PPI) analysis (gene = 12), gene expression analysis (n = 24) by clinical samples of DCs from the gse26887 dataset, biological process (BP) analysis (FDR ≤ 0.05, gene = 7), KEGG pathway analysis (FDR ≤ 0.05, gene = 7), and ingredient target pathway network analysis (gene = 7) by applying these targets from the screen, Biological processes, disease pathways regulated by targets and the relationship between each component target and pathway were obtained. We further screened the targets and visualized the docking results by precision molecular docking of ingredients and targets, after which we performed molecular dynamics simulation and consulted a large number of relevant literatures for validation of the results.

Results

Through screening, analysis and validation of the data, we finally confirmed the presence of 36 active ingredients in HQ, RS, GG, and SY, which mainly act on AKT1, ADRB2, GSK3B, PPARG, and BCL2 targets, and these five targets mainly regulate PI3K-Akt, Adrenergic signaling in cardiomyocytes, AGE-RAGE signaling pathway in diabetic complications, JAK-STAT, cGMP-PKG, AMPK, and mTOR signaling pathway exert preventive or therapeutic effects on DCM. Molecular dynamics (MD) simulations revealed that the complex formed by Calycosin, Frutinone A, Puerarin, Inophyllum E, the four active components of HQ, RS, GG, and SY, and the four target proteins ADRB2, PPARG, AKT1, and GSK3B acting on DCS is able to exist in a very stable tertiary structure under human environment.

Conclusions

our study successfully explains the effective mechanism of HQ, RS, GG, and SY in ameliorating DC, while predicting the potential targets and active components of HQ, RS, GG, and SY in treating DC, which provides a new basis for investigating novel mechanisms of action at the network pharmacology level and a great support for subsequent DC research.

1. Introduction

Diabetic cardiomyopathy (DC) is a pathophysiological condition of diabetes mellitus (DM)-induced, and human DC has become a well-documented disease since Shirley Rubler identified a novel cardiomyopathy called DC in diabetic patients in 1972 [1, 2]. Studies have shown that in type 2 diabetes, the risk of heart disease induced by hyperglycemia and insulin resistance increases 2–8 times, and 19% of patients with heart failure symptoms appear [3]. Under such high incidence rate of DC, the relevant treatment strategies are reported, a large part of which belong to the gene targeting regulatory pathway.

It is undeniable that most glucose related pathological processes in the human body are related to hyperglycemia. Among them, the impaired signal transduction pathway of cardiac insulin metabolism is a key pathophysiological process related to diabetic cardiomyopathy [4]. This signal transduction pathway is mammalian target of rapamycin (mTOR) signaling pathway. Studies have shown that activation of mTOR signaling pathway can lead to damage of PI3K-Akt signaling pathway and indirectly reduce glucose uptake. Thus, the intracellular Ca^{2+} level and its sensitivity in cardiomyocytes are increased through cGMP PKG signaling pathway [4]. In fact, hyperglycemia and gluconic acid toxicity can induce protein glycosylation reaction, resulting in the increase of advanced glycation end products (ages), which in turn leads to the cross-linking of cardiac connective tissue, the impairment of cardiac stiffness and relaxation [4]. Ages may bind to its cell surface receptor (RAGE) to indicate maladaptive inflammatory gene expression, thereby increasing matrix proteins through processes mediated by Janus kinase (JAK) in blood vessels and heart tissues [4]. Some studies have also shown that the activation of ages-rage signaling pathway can promote NF- κ B activation, which in turn increases the expression of proinflammatory cytokines and cardiac fibrosis [5]. Therefore, effectively inhibiting the formation of ages and ages-rage signaling pathway can prevent myocardial fibrosis and reduce the symptoms of DC.

At present, the drug Rybelsus (GLP-1 receptor agonist, DPP4 inhibitor) can effectively treat type two diabetes and some complications, and its side effects are small. However, there are different opinions on the impact of intensive blood glucose control with various hypoglycemic drugs on cardiovascular related diseases [6, 7], although there are reports, ω-3 fatty acid combined with metformin has a certain effect on diabetic cardiomyopathy, but does not prove that this method is effective for human DC[8]. Therefore, these studies are in the exploratory stage. For the complete cure of DC, there still need a lot of theoretical and basic scientific research.

In this study, through network pharmacology, we found many components that can effectively treat or prevent DC in four traditional Chinese medicines: HQ, RS, GG, and SY for the first time. Among them, the representative components are Puerarin (in GG), Calycosin (in HQ), Inophyllum E (in SY), and Frutinone A (in RS), Our findings are consistent with the conclusions of previous studies (Puerarin [9, 10], and Calycosin [11, 12], etc.). However, most of these studies are carried out around the usual basic experimental methods, which are different from those of others. Our research is based on computer deep learning model and other means, using improved network pharmacology process to simulate the existing state of these compounds in standard human environment after binding with their target proteins, then select the most suitable effective components of traditional Chinese medicine for the treatment or prevention of DC.

2. Materials And Methods

2.1 Screening of active components of four traditional Chinese medicines

TCMSP, traditional Chinese Medicine System Pharmacology database (https://tcmsp-e.com/) [13] It is one of the most commonly used databases for screening active components of traditional Chinese medicine. Its advantage is that the database gives the parameters of compound relative molecular weight (MW), oral bioavailability (OB) and drug similarity (DL). These parameters play a very important role in the evaluation of drug efficacy. Only when these parameters exceed a certain value (MW ≥ 180kda, OB > 0 and DL ≥ 0.18 or OB > 70% and DL ≥ 0), can effectively reflect the class properties of a component.

2.2 Acquisition of targets of traditional Chinese medicine and DC

In order to study the mechanism of active ingredients of HQ, RS, GG, and SY targeting DC, firstly, we must obtain the targets that all active ingredients can act on. Secondly, we need to obtain the targets of DC verified by experiments. Only by finding the common part of these two kinds of targets can we continue to study the experiment.

We searched the above obtained active components of HQ, RS, GG, and SY in TCMSP database, obtained all targets corresponding to the chemical components of traditional Chinese medicine, and compared them with (https://www.disgenet.org/) [14] the obtained DC targets are combined in Disgenet database and Venn intersection is taken to obtain the disease target information we finally need.

2.3 Construction of PPI network and C-T-D network

To obtain disease targets with interaction relationship, we performed protein interaction analysis (PPI analysis) on all targets obtained by intersection. We preset the required minimum interaction score of 0.400 analysis conditions. Through PPI network analysis, we obtained the interaction relationship network of all proteins. According to this network diagram, we obtained the preliminarily screened DC targets.

In order to clearly show the corresponding relationship between the four traditional Chinese medicines and their active components, targets and DC, we use Cytoscape 3.8.0 software [15] to construct the component target disease network for the above active components and targets, and obtain the C-T-D relationship diagram we need. In this network diagram, we use different node shapes and colors to represent each content. So far, we have completed the preliminary screening of the active ingredients related to the treatment of DC with traditional Chinese medicine.

2.4 Geo gene expression analysis

Different from TCGA database, it comes from the geo database of NCBI (https://www.ncbi.nlm.nih.gov/geo/) It not only contains cancer-related clinical information, but also has many non-cancer clinical information, which makes the geo database more perfect in the provision of clinical case information.

To further screen the active ingredients and their targets that we have preliminarily screened, we obtained enough DC clinical case samples from the GSE26887 data set (GPL6244 platform) of GEO database (the data set contains 24 clinical samples related to human DC memory expression). Through the gene expression difference analysis of GSE clinical samples, we drew an intuitive heat map of gene expression and screened the targets again.

2.5 C-T-P network and gene enrichment analysis

In order to evaluate the interaction between the targets screened above, protein interaction network and active ingredient target pathway network (C-T-P network) were constructed. In order to explore the biological processes and pathways involved by each target in vivo, through string database (https://cn.string-db.org) [16] After retrieving the data of target genes, we carried out biological process (BP) analysis in GO (gene ontology) analysis and KEGG (Kyoto Encyclopedia of genes and genes) enrichment analysis. Among them, the FDR of go analysis is ≤ 0.05, and

the FDR of KEGG enrichment analysis is under 0.05, which meets the requirements and statistical significance of significant gene enrichment in vivo.

FDR value is the correction of P value, and the screening results are more accurate. Therefore, this step aims to obtain the biological process and in vivo pathway of target action, which provides a basis for subsequent research.

2.6 Molecular docking

Molecular docking is a method of drug design through the characteristics of receptors and the interaction between receptors and drug molecules. A theoretical simulation method to study the interaction between molecules (such as ligands and receptors) and predict their binding mode and affinity. In recent years, molecular docking method has become an important technology in the field of computer-aided drug research [17].

The precise molecular docking between the effective components of traditional Chinese medicine and DC targets is carried out through tools such as autodock Vina [18] and PyMOL software [19]. The binding energy between the components and targets is first used to verify whether the effect of the effective components of four traditional Chinese medicines on DC is reliable, and further exclude the components with poor effect on DC in HQ, RS, GG, and SY.

2.7 Molecular dynamics simulation verification

On the basis of molecular docking and GSE gene difference analysis, we carried out molecular dynamics simulation (MD simulation) [20] to verify the results. MD simulation is a means to simulate the movement of small molecules in the body environment by computer. We carried out MD simulation with GROMACS software [21], set the physical conditions as constant temperature (310K), constant pressure (101kpa) and periodic boundary conditions, and used TIP3P water model, Simulate the human environment in 0.145mol/l neutral sodium chloride solution.

After the state balance of all environments, we use the screened component target complex system for 50ns MD simulation, in which the conformation storage calculation is carried out every 10ps. The RMSD (root mean square deviation), RMSF (root mean square flux) of MD simulation results the radius of gyration analysis and visualization are carried out using GROMACS embedded program and VMD. We know that the gyration radius RG of protein reflects the volume and structural state of protein macromolecules. The larger the RG value of the same system, the expansion of the system occurs in the process of MD.

3. Results

3.1 Screening results of active components of traditional Chinese Medicine

We collected 53, 80, 14, and 172 known active components of HQ, RS, GG, and SY from TCMSP database, including alkaloids, lipids, flavonoids and flavonoids. On the premise of MW ≥ 180kda unchanged, we screened 17, 10, 9, and 20 effective drug-like components from four traditional Chinese medicine compounds under two screening conditions of OB > 0 and DL ≥ 0.18 or OB > 70% and DL ≥ 0, The screening details of these components are shown in (Table 1).

Table 1
Screening information of active compounds in four traditional Chinese medicines

Herb	Mol ID	PubChem CID	Molecule Name	MW	AlogP	OB(%)	DL
HUANG QI	MOL000098	5280343	Quercetin	302.25	1.504	46.43335	0.27525
HUANG QI	MOL000239	5318869	Jaranol	314.31	2.087	50.82882	0.29148
HUANG QI	MOL000251	5320946	Rhamnocitrin	300.28	2.022	12.89912	0.26607
HUANG QI	MOL000354	5281654	Isorhamnetin	316.28	1.755	49.60438	0.306
HUANG QI	MOL000371	15689655	3,9-Di-O-Methylnissolin	314.36	2.892	53.74153	0.47573
HUANG QI	MOL000378	15689652	7-O-Methylisomucronulatol	316.38	3.379	74.68614	0.29792
HUANG QI	MOL000380	14077830	10-Methoxymedicarpin	300.33	2.641	64.25545	0.42486
HUANG QI	MOL000390	5281708	Daidzein	254.25	2.332	19.44106	0.18694
HUANG QI	MOL000391	442813	Ononin	430.44	0.678	11.52206	0.7756
HUANG QI	MOL000392	5280378	Formononetin	268.28	2.583	69.67388	0.21202
HUANG QI	MOL000412	442811	Mucronulatol	302.35	3.128	4.215732	0.26462
HUANG QI	MOL000415	5280805	Rutin	610.57	-1.446	3.201533	0.68283
HUANG QI	MOL000416	332427	Lariciresinol	360.44	2.463	5.526192	0.37941
HUANG QI	MOL000417	5280448	Calycosin	284.28	2.316	47.75183	0.24278
HUANG QI	MOL000422	5280863	Kaempferol	286.25	1.771	41.88225	0.24066
HUANG QI	MOL000433	135398658	Folic Acid	441.45	0.007	68.96044	0.7057
HUANG QI	MOL000436	6603886	Zinc3869607	256.27	2.9	87.50845	0.14769
REN SHEN	MOL000422	5280863	Kaempferol	286.25	1.771	41.88225	0.24066
REN SHEN	MOL000787	4970	Fumarine	353.4	2.953	59.2625	0.82694
REN SHEN	MOL003648	91510	Inermin	284.28	2.442	65.83093	0.53754

Herb	Mol ID	PubChem CID	Molecule Name	MW	AlogP	OB(%)	DL
REN SHEN	MOL005305	5317284	Nepetin	316.28	2.051	26.75038	0.30835
REN SHEN	MOL005321	441965	Frutinone A	264.24	2.699	65.90373	0.34184
REN SHEN	MOL005344	119307	Ginsenoside Rh2	622.98	4.043	36.31951	0.55868
REN SHEN	MOL005356	96943	Girinimbin	263.36	4.597	61.2153	0.31484
REN SHEN	MOL005384	132350840	Suchilactone	368.41	3.731	57.51882	0.55573
REN SHEN	MOL007500	73599	Panaxatriol	476.82	4.286	15.41984	0.79324
REN SHEN	MOL011400	441922	Ginsenoside Rf	801.14	1.127	17.74108	0.24146
GE GEN	MOL000390	5281708	Daidzein	254.25	2.332	19.44106	0.18694
GE GEN	MOL000391	442813	Ononin	430.44	0.678	11.52206	0.7756
GE GEN	MOL000392	5280378	Formononetin	268.28	2.583	69.67388	0.21202
GE GEN	MOL000481	5280961	Genistein	270.25	2.065	17.93288	0.21384
GE GEN	MOL001999	8417	Scoparone	206.21	1.867	74.75496	0.086914
GE GEN	MOL002959	5319422	3'-Methoxydaidzein	284.28	2.316	48.56909	0.24261
GE GEN	MOL004631	5466139	8-Hydroxydaidzein	270.25	2.065	20.66807	0.21583
GE GEN	MOL009720	107971	Daidzin	416.41	0.428	14.31529	0.72537
GE GEN	MOL012297	5281807	Puerarin	416.41	-0.06	24.0309	0.69099
SANG YE	MOL000098	5280343	Quercetin	302.25	1.504	46.43335	0.27525
SANG YE	MOL000207	7127	Methyleugenol	178.25	2.805	73.36011	0.042845
SANG YE	MOL000251	5320946	Rhamnocitrin	300.28	2.022	12.89912	0.26607
SANG YE	MOL000415	5280805	Rutin	610.57	-1.446	3.201533	0.68283
SANG YE	MOL000422	5280863	Kaempferol	286.25	1.771	41.88225	0.24066

Herb	Mol ID	PubChem CID	Molecule Name	MW	AlogP	OB(%)	DL
SANG YE	MOL000433	135398658	Folic Acid	441.45	0.007	68.96044	0.7057
SANG YE	MOL000561	5282102	Astragalin	448.41	-0.32	14.02685	0.73616
SANG YE	MOL000842	5988	Sucrose	342.34	-4.311	7.170823	0.2273
SANG YE	MOL002902	5317238	Ethyl Caffeate	208.23	1.967	103.8508	0.067883
SANG YE	MOL003759	5491637	Iristectorigenin A	330.31	2.032	63.36362	0.33929
SANG YE	MOL003767	5281811	Tectorigenin	300.28	2.048	28.40992	0.26822
SANG YE	MOL003847	5254	Inophyllum E	402.47	4.664	38.80967	0.85408
SANG YE	MOL003857	155248	Moracin C	310.37	4.998	82.13155	0.28665
SANG YE	MOL003858	641378	Moracin D	308.35	4.196	60.92843	0.38454
SANG YE	MOL003859	5319888	Moracin E	308.35	4.196	56.07638	0.38469
SANG YE	MOL003861	5319890	Moracin G	308.35	4.516	75.77745	0.4224
SANG YE	MOL003879	5281725	4-Prenylresveratrol	296.39	4.871	40.53872	0.20818
SANG YE	MOL004881	9862769	Morachalcone A	340.4	4.489	1.360696	0.30435
SANG YE	MOL007879	631170	Tetramethoxyluteolin	342.37	3.071	43.68476	0.37009

3.2 Acquisition of intersection targets and construction results of PPI network

After screening the active ingredients, we obtained 220 DC non repetitive targets (disease ID: C0853897) by using the latest DC target data in the Disgenet database. Then, through the intersection of four traditional Chinese medicines and DC targets, we obtained the Venn diagram of the number of overlapping targets of HQ, RS, GG, and SY with DC (Fig. 1). In the Venn diagram, there are 12 overlapping targets of four traditional Chinese medicines and DC at the same time. See Table 2 for the 12 overlapping targets.

Table 2
12 intersection targets of four traditional Chinese medicines and DC

Coincident targets	Uniprot ID
BCL2	P10415
CASP9	P55211
CASP3	P42574
CASP8	Q14790
GSK3B	P49841
AKT1	P31749
PPARG	P37231
DPP4	P27487
AHSA1	O95433
ADRB2	P07550
MMP9	P14780
IL1B	P01584

In order to obtain disease targets with interaction relationship, we conducted PPI network analysis on the 12 preliminarily screened targets. Therefore, we obtained the interaction network diagram of proteins encoded by 12 genes (Fig. 2), from which we obtained DC targets after further screening.

We can clearly see that in Fig. 2, multiple targets interact most strongly, such as apoptosis regulator Bcl-2 (BCL2), matrix metalloproteinase-9 (MMP9), Caspase-8 (CASP8), caspase-3 (CASP3), caspase-9 (CASP9), peroxisome promoter activated receiver gamma (PPARG), glycogen synthase kinase-3 beta (GSK3B) and beta-2 regenerative receiver (ADRB2).

3.3 The results of C-T-D network construction and GSE gene expression analysis

In order to map the active components of four traditional Chinese medicines and their relationship with 12 intersection targets of DC one by one, we used Cytoscape to construct C-T-D network (Fig. 3), which contains 63 nodes and 180 edges. Through the C-T-D network, we can find that the components of HQ, RS, GG, and SY with strong or weak effect on the target rank 5280343 (Quercetin), 5280863 (Kaempferol), 5491637 (Iritectorigenin A), 5281725 (4-prenylresveratrol), 631170 (Tetramethoxyluteolin) and 15689652 (7-o-methylisocronulatol) respectively. However, this does not mean that these components are really effective, so we need to continue the screening experiment.

To ensure the accuracy of the experimental data, we further screened the components and targets. Through the geo database, we obtained a total of 32321 DC related disease genes from the gse26887 data set. It is undeniable that these DC gene expression data have high reference value. These genes correspond to the clinical samples of 24 DCS

in the gse26887 data set, we selected the expression data of 12 genes we need from these 24 DC case samples, and then drew the gene expression heat map using R4.0.2 visual programming language (Fig. 4).

According to the gene difference analysis of GSE clinical samples, we excluded 5 targets without significant difference from the remaining 12 targets, and the remaining 7 DC differential expression targets. The expression levels of these 7 targets from high to low are AKT1, GSK3B, AHSA1, PPARG, CASP9, BCL2, and ADRB2, especially AKT1, GSK3B, and AHSA1, which are significantly higher than other targets in DC patients. After matching these seven targets with the active components of HQ, RS, GG, and SY, we screened more accurate components from the active components of their respective traditional Chinese medicine.

3.4 GO (BP) and KEGG enrichment analysis

According to the gene difference analysis of GSE clinical samples, we used the screened seven DC differential expression targets, which are AKT1, GSK3B, AHSA1, PPARG, CASP9, BCL2 and ADRB2. We used string database to analyze the go biological process (BP) of these targets, and drew a chord diagram representing 25 biological regulation processes (Fig. 5).

Through the biological process of GO enrichment analysis, it can be seen that AKT1, ADRB2, and PPARG of the seven DC targets selected by us can regulate the blood circulation process, and GSK3B, BCL2, and AKT1 can regulate the mitochondrion organization, negative regulation of intracellular signal transmission and negative regulation of exogenous signaling pathway, these processes are associated with diabetic cardiomyopathy.

To ensure the reliability and statistical significance of the data, we performed KEGG enrichment analysis in the string database with FDR < 0.02, and showed 20 pathways in the comprehensive results in the form of bubble chart (Fig. 6).

After analyzing 20 KEGG pathways, we found that KEGG enrichment analysis revealed many DC related pathways, which were mainly enriched in EGFR tyrosine kinase inhibitor resistance, PI3K-Akt signaling pathway, Adrenergic signaling in cardiocytes, AGE-RAGE signaling pathway in diabetic complications, HIF-1 signaling pathway, AMPK signaling pathway MTOR signaling pathway and cGMP-PKG signaling pathway.

3.5 Analysis of C-T-P network construction results

Referring to the results of KEGG enrichment analysis, in order to make it easy to understand, we connected the components, 7 targets and 20 pathways of the screened four traditional Chinese medicines of HQ, RS, GG, and SY, and constructed a C-T-P network diagram (Fig. 7), so as to visualize the relationship between components and targets and the relationship between targets and pathways. A total of 70 nodes and 171 edges of C-T-P network were obtained.

3.5 Analysis of molecular docking results

Through the above series of analysis, screening and verification, we have determined the target sites of 39 components of the four traditional Chinese medicines, of which these 39 components can act on multiple targets of DC. However, even by observing the corresponding relationship and the known effects of the targets, we can infer that they are Puerarin, Quercetin, Frutinone A, Calycosin, Inophyllum E, Kaempferol, 8-hydroxydaidzein 4-prenylresveratrol, Moracin e, Morachalcone A, and Daidzein may all be effective drugs for DC treatment, but further experiments are needed to verify our conjecture.

After obtaining this information, we use ChemDraw 19.0 software [22] to draw the structure of six components, save it as mol2 file and use PDB (https://www.rcsb.org/) database [23] selects the corresponding tertiary structure of the

protein with ligand according to the structure of the component, downloads the pdb file, processes the PDB protein file through PyMOL (removing water molecules and redundant structures, etc.), saves the two file formats as pdbqt file using autodock software, selects the ligand and coordinate position (x, y, z), and screens and sorts the components through the distance of hydrogen bond, These three-level structures are predicted by X-ray diffraction method. Then, we used autodock and autodock Vina for molecular docking between components and targets. The docking results are shown in Table 3. We sorted the docking results, and then selected 9 of the 18 pairs of component target complexes with binding energy ≤-9.1kcal/mol for PyMOL treatment to visualize the results (Fig. 8).

Table 3
Molecular docking results of active components of four traditional Chinese medicines and DC targets

Herb	Compounds	PubChem CID	Targets	Affinity (kcal/mol)	PDB ID
GE GEN	5281807	Puerarin	AKT1	-10.7	6HHF
REN SHEN	441965	Frutinone A	ADRB2	-10.5	2RH1
HUANG QI	5280448	Calycosin	ADRB2	-9.9	2RH1
SANG YE	5254	Inophyllum E	GSK3B	-9.9	2X39
REN SHEN	441965	Frutinone A	PPARG	-9.7	3SZ1
SANG YE	641378	Moracin D	GSK3B	-9.7	2X39
GE GEN	5466139	8-Hydroxydaidzein	PPARG	-9.2	3SZ1
GE GEN	5280961	Genistein	AKT1	-9.1	6HHF
HUANG QI	5280343	Quercetin	AKT1	-9.1	6HHF
HUANG QI	5280863	Kaempferol	AKT1	-9.1	6HHF
HUANG QI	5281654	Isorhamnetin	PPARG	-9.1	3SZ1
REN SHEN	5280863	Kaempferol	AKT1	-9.1	6HHF
SANG YE	5281725	4-Prenylresveratrol	ADRB2	-9.1	2RH1
SANG YE	5280343	Quercetin	AKT1	-9.1	6HHF
SANG YE	5280863	Kaempferol	AKT1	-9.1	6HHF
SANG YE	5319888	Moracin E	GSK3B	-9.1	2X39
SANG YE	5319888	Moracin E	PPARG	-9.1	3SZ1
SANG YE	9862769	Morachalcone A	PPARG	-9.1	3SZ1
HUANG QI	5280448	Calycosin	PPARG	-9.0	3SZ1
SANG YE	631170	Tetramethoxyluteolin	ADRB2	-9.0	2RH1
GE GEN	5281708	Daidzein	PPARG	-8.9	3SZ1
HUANG QI	5281708	Daidzein	PPARG	-8.9	3SZ1
REN SHEN	4970	Fumarine	ADRB2	-8.9	2RH1
HUANG QI	5280448	Calycosin	GSK3B	-8.8	2X39
REN SHEN	91510	Inermin	ADRB2	-8.8	2RH1
GE GEN	5319422	3'-Methoxydaidzein	GSK3B	-8.7	2X39
HUANG QI	14077830	10-Methoxymedicarpin	ADRB2	-8.7	2RH1
SANG YE	5319890	Moracin G	GSK3B	-8.7	2X39

Herb	Compounds	PubChem CID	Targets	Affinity (kcal/mol)	PDB ID
GE GEN	107971	Daidzin	GSK3B	-8.6	2X39
HUANG QI	6603886	ZINC3869607	ADRB2	-8.6	2RH1
SANG YE	5281811	Tectorigenin	PPARG	-8.5	3SZ1
HUANG QI	6603886	ZINC3869607	GSK3B	-8.4	2X39
HUANG QI	135398658	Folic Acid	GSK3B	-8.4	2X39
HUANG QI	5280343	Quercetin	PPARG	-8.4	3SZ1
HUANG QI	5320946	Rhamnocitrin	PPARG	-8.4	3SZ1
SANG YE	135398658	Folic Acid	GSK3B	-8.4	2X39
SANG YE	5281811	Tectorigenin	GSK3B	-8.4	2X39
SANG YE	5280343	Quercetin	PPARG	-8.4	3SZ1
SANG YE	5320946	Rhamnocitrin	PPARG	-8.4	3SZ1
GE GEN	5280378	Formononetin	ADRB2	-8.3	2RH1
GE GEN	442813	Ononin	PPARG	-8.3	3SZ1
GE GEN	107971	Daidzin	PPARG	-8.3	3SZ1
HUANG QI	5280378	Formononetin	ADRB2	-8.3	2RH1
HUANG QI	442813	Ononin	PPARG	-8.3	3SZ1
HUANG QI	5280863	Kaempferol	PPARG	-8.3	3SZ1
REN SHEN	5280863	Kaempferol	PPARG	-8.3	3SZ1
SANG YE	5280863	Kaempferol	PPARG	-8.3	3SZ1
GE GEN	5280378	Formononetin	GSK3B	-8.2	2X39
GE GEN	5280378	Formononetin	PPARG	-8.2	3SZ1
HUANG QI	5280378	Formononetin	GSK3B	-8.2	2X39
HUANG QI	5281654	Isorhamnetin	GSK3B	-8.2	2X39
HUANG QI	5280378	Formononetin	PPARG	-8.2	3SZ1
SANG YE	641378	Moracin D	PPARG	-8.2	3SZ1
GE GEN	5281807	Puerarin	PPARG	-8.1	3SZ1
HUANG QI	442811	Mucronulatol	GSK3B	-8.1	2X39
REN SHEN	96943	Girinimbin	ADRB2	-8.1	2RH1
GE GEN	5281807	Puerarin	GSK3B	-8.0	2X39
GE GEN	5319422	3'-Methoxydaidzein	PPARG	-8.0	3SZ1

Herb	Compounds	PubChem CID	Targets	Affinity (kcal/mol)	PDB ID
SANG YE	5281725	4-Prenylresveratrol	GSK3B	-8.0	2X39
SANG YE	9862769	Morachalcone A	GSK3B	-8.0	2X39
HUANG QI	332427	Lariciresinol	ADRB2	-7.9	2RH1
SANG YE	5491637	Iristectorigenin A	GSK3B	-7.9	2X39
HUANG QI	5320946	Rhamnocitrin	GSK3B	-7.8	2X39
SANG YE	5320946	Rhamnocitrin	GSK3B	-7.8	2X39
SANG YE	631170	Tetramethoxyluteolin	GSK3B	-7.8	2X39
SANG YE	5281725	4-Prenylresveratrol	PPARG	-7.8	3SZ1
SANG YE	155248	Moracin C	PPARG	-7.8	3SZ1
GE GEN	5280961	Genistein	BCL2	-7.6	6GL8
HUANG QI	15689652	7-O-Methylisomucronulatol	ADRB2	-7.6	2RH1
SANG YE	5491637	Iristectorigenin A	PPARG	-7.6	3SZ1
SANG YE	631170	Tetramethoxyluteolin	PPARG	-7.6	3SZ1
GE GEN	5281708	Daidzein	ADRB2	-7.5	2RH1
HUANG QI	5281708	Daidzein	ADRB2	-7.5	2RH1
HUANG QI	6603886	ZINC3869607	PPARG	-7.5	3SZ1
HUANG QI	5280343	Quercetin	ADRB2	-7.4	2RH1
HUANG QI	15689652	7-O-Methylisomucronulatol	PPARG	-7.4	3SZ1
SANG YE	5280343	Quercetin	ADRB2	-7.4	2RH1
GE GEN	8417	Scoparone	ADRB2	-7.1	2RH1
GE GEN	5280961	Genistein	PPARG	-7.1	3SZ1
REN SHEN	132350840	Suchilactone	ADRB2	-7.1	2RH1
HUANG QI	15689655	3,9-Di-O-Methylnissolin	ADRB2	-7.0	2RH1
HUANG QI	15689652	7-O-Methylisomucronulatol	GSK3B	-7.0	2X39
HUANG QI	442811	Mucronulatol	PPARG	-7.0	3SZ1
GE GEN	5281807	Puerarin	BCL2	-6.7	6GL8
SANG YE	5317238	Ethyl Caffeate	ADRB2	-6.7	2RH1
GE GEN	5281807	Puerarin	CASP9	-6.6	1NW9
HUANG QI	5280343	Quercetin	BCL2	-6.5	6GL8
SANG YE	5280343	Quercetin	BCL2	-6.5	6GL8

Herb	Compounds	PubChem CID	Targets	Affinity (kcal/mol)	PDB ID
HUANG QI	5280863	Kaempferol	AHSA1	-6.4	7DMD
REN SHEN	5280863	Kaempferol	AHSA1	-6.4	7DMD
SANG YE	5280863	Kaempferol	AHSA1	-6.4	7DMD
HUANG QI	5280863	Kaempferol	BCL2	-6.3	6GL8
REN SHEN	5280863	Kaempferol	BCL2	-6.3	6GL8
SANG YE	5280863	Kaempferol	BCL2	-6.3	6GL8
HUANG QI	5280343	Quercetin	AHSA1	-6.0	7DMD
SANG YE	5280343	Quercetin	AHSA1	-6.0	7DMD
SANG YE	5988	Sucrose	PPARG	-5.9	3SZ1
GE GEN	5280961	Genistein	AHSA1	-5.8	7DMD
GE GEN	5280961	Genistein	CASP9	-5.8	1NW9
HUANG QI	5280343	Quercetin	CASP9	-5.8	1NW9
SANG YE	5280343	Quercetin	CASP9	-5.8	1NW9
SANG YE	7127	Methyleugenol	ADRB2	-5.0	2RH1

To ensure the availability and reference value of the data, we set the coordinates (x, y, z) according to the structural size of the component itself. It is known that the larger the value in the coordinates, the greater the affinity of docking and the greater the affinity. It is proved that the closer the combination between the component and the target, the more effective the component is. Therefore, these coordinate values we use are the most appropriate for the component itself. The docking results showed that the average binding energy (kcal/mol) between the component and the target was about − 7.96 kcal/mol, of which the best binding energy was − 10.7 kcal/mol and the worst was − 5.0 kcal/mol.

Through the visualization results, we can know that the binding energy between 37 of the 39 effective components of traditional Chinese medicine and DC target is less than-7.0 kcal/mol, which means that the four traditional Chinese medicines of HQ, RS, GG, and SY have great therapeutic potential for DC. Among the six pairs of component target complexes with binding energy ≤-9.7 kcal/mol, four representative pairs are Puerarin-AKT1, Calycosin-ADRB2, Inophyllum E-GSK3B, and Frutinone A-PPARG. Puerarin can bind to amino acid residues TRY-272, THR-81, THR-82, and GLN-79 of AKT1 protein, and the average hydrogen bond distance is 2.725Å. Calycosin can bind to amino acid residues THR-118, VAL-114, TRY-308, PHE-193 THR-195, and SER-203, and the average hydrogen bond distance is about 2.8Å, which means that perhaps Puerarin and Calycosin are similar to the stable type of the complex bound to the target, respectively. Inophyllum E can bind to the amino acid residue ASP-275 of GSK3B protein with a hydrogen bond distance of about 3.4Å. Frutinone a can bind to the amino acid residues SER-342 and HIS-266 of PPARG protein with an average hydrogen bond distance of about 3.35Å, which means that the stable types of the complexes bound to the target by Puerarin and Calycosin are similar.

3.6 Analysis of MD simulation results

The result data of MD such as RMSD, RMSF and RG values are an important basis to measure the stability of the complex system of components and proteins and the stability of the tertiary structure of proteins combined with small molecules. Therefore, we selected four representative pairs of Puerarin-AKT1, Calycosin-ADRB2, Inophyllum E-GSK3B, and Frutinone A-PPARG from the six pairs of component target complexes with binding energy ≤-9.7 kcal/mol for MD simulation verification. In order to make these data more intuitive in front of us, we visualized their output data (Fig. 9).

From the results of MD simulation, we can see that in the four MD systems of composition and target complex, the overall performance of Puerarin and AKT1 complex system is poor, including large fluctuation of RMSD, large radius of gyration and small floating consistency of RMSF. These situations mean that the system can only show very weak inhibition against DC.

For the two complex systems of Inophyllum E-GSK3B and Frutinone A-PPARG, we can observe that among the three experimental results of RMSD, RG, and RMSF, Frutinone A-PPARG system has better protein hydrophobicity and more stable tertiary structure than the system formed by Inophyllum E-GSK3B, but the performance of these two systems is very good. This result is very intuitive. The binding energy data of these two systems are also very ideal, that is, PPARG and GSK3B are possible as new therapeutic targets of DC. We have made it clear that Frutinone A and Inophyllum E, the components of RS and SY, can well target DC highly expressed proteins.

In terms of RMSD, RG and RMSF, the MD system formed by Calycosin-ADRB2 shows an excellent state, that is, the system can exist stably without affecting its own and other protein structures. The system has the most stable RMSD and generally stable RG value (the system will not expand) and it is obvious that the system is undoubtedly the best in all aspects.

Therefore, Calycosin, Frutinone A, Puerarin, and Inophyllum E, the four active components of HQ, RS, GG, and SY, can play a role in improving or treating DC to a certain extent after acting on the four target proteins ADRB2, PPARG, AKT1, and GSK3B.

4. Discussion

4.1 The role of PI3K-Akt pathway in DC

As an important complication of diabetes, DC is thought to be caused by insulin resistance (IR) in cardiac myocytes. Therefore, improving the IR state of cardiomyocytes may be a way to treat DC. In recent years, the PI3K-Akt signaling pathway has become an important pathway for the treatment of cardiovascular diseases and some metabolic diseases, such as type 2 diabetes. Studies have shown that activation of PI3K-Akt signaling pathway can improve the level of IR in cardiomyocytes [24], which has been described in the introduction section.

However, activation of the PI3K-Akt pathway alone is not enough to treat the symptoms of diabetic cardiomyopathy. The researchers divided the diabetic rats with continuous high-fat diet and streptozotocin into 5 groups, namely, the normal control group (1 groups), the untreated diabetes group (1 groups) and the diabetes group (3 groups). The rats in the diabetic group were treated with Da gliclazide for periodic treatment. The results showed that the PI3K-Akt, JAK2-STAT5, and ERK-MAPK signaling pathways in the untreated diabetic group all had a downward trend, whereas on the contrary, the rats in the diabetic group had a down-regulation. The downregulation of the above three pathways in the three groups of rats treated with dapagliflozin was weakened [25], which means that the

simultaneous activation of PI3K-Akt, JAK2-STAT5, and ERK-MAPK signaling pathways can relatively effectively treat DC.

4.2 Evidence of Puerarin in the treatment of DC

Puerarin is a natural glycoside flavonoid active compound. A few years ago, Puerarin was believed to have potential antioxidant, anti-inflammatory, or anti apoptotic mechanisms, which can effectively alleviate chronic alcohol induced liver injury [26, 27] and treat STZ mediated diabetes [28]. Therefore, we speculate that Puerarin has a certain possibility in the treatment of DC. We found that the researchers used Puerarin ultrasound microbubble contrast agent (PMBs) in the treatment of diabetic cardiomyopathy, and the results showed that PMBs is a promising target drug delivery system and a new non-invasive strategy for the treatment of diabetic cardiomyopathy [10].

In addition, the researchers found that Puerarin combined with HQ injection also found the great potential of Puerarin in the treatment of DC, that is, HQ injection combined with Puerarin could inhibit the endoplasmic reticulum stress signal molecule IRE1 in the heart tissue of type 2 diabetic mice to a certain extent. α the expression of XBP1 can alleviate endoplasmic reticulum stress and protect the heart function of type 2 diabetic mice [29].

5. Conclusion

Our research shows that Puerarin, a component of GG, can target AKT1, PPARG, GSK3B, BCL2, and CASP9. After MD verification, it is found that the complex of Puerarin and AKT1 can exist stably, that is, Puerarin can positively regulate the expression of AKT1, and then regulate PI3K-Akt signaling pathway to treat or improve the symptoms of DC. Of course, this does not mean that other compounds we found have no effect. On the contrary, the effect of other compounds on DC may be better and more obvious than Puerarin. Taking them together with HQ, RS, GG, or SY decoction may be more effective than any existing medical means. However, the existing research on other compounds in this field is not enough to support our view. Therefore, the complete cure of DC patients can't be completed by one person or a small team, which still needs the joint efforts of researchers in various fields.

Declarations

Acknowledgements

Not applicable.

Authors' contributions

Xingchen Guo and Wanhao Gao contributed equally to this research and Xingchen Guo and Wanhao Gao wrote the main manuscript text.Xingchen Guo and Dongdong Zhang prepared all figures. Dongdong Zhang and Muwei Li are corresponding authors. All authors reviewed the manuscript.The author(s) read and approved the final manuscript.

Authors:Xingchen Guo and Wanhao Gao contributed equally to this work.Department of Cardiology, People's Hospital of Zhengzhou University, Zhengzhou University, Zhengzhou, China.

Corresponding author:Dongdong Zhang,School of life sciences, Shihezi University, Xiangyang street, Shihezi 832003, PR China. Muwei Li*, Department of Cardiology, People's Hospital of Zhengzhou University, No.7 Weiwu Road, Zhengzhou, Henan, 450003, PR. China. Heart center of Henan Provincial People's Hospital, No.1 Fuwai Road, Zhengdong New District, Zhengzhou, Henan, 450018, PR China.

E-mail addresses:15136159648@163.com(Xingchen Guo), gaohaoemail@163.com(Wanhao Gao), sedate@stu.shzu.edu.cn(Dongdong Zhang), lmw0207zzu@163.com(Muwei Li)

Funding

Not applicable.

Availability of data and materials

The datasets generated and/or analysed during the current study are not publicly available due the limited scope of data availability,these data are used under the license of this study and are not disclosed,but are available from the authors [15136159648@163.com(Xingchen Guo) and sedate@stu.shzu.edu.cn(Dongdong Zhang)] on reasonable request.

Ethics approval and consent to participate

Not applicable.

Consent for publication

Not applicable.

Competing interests

Not applicable.

References

1. Dillmann W. H. (2019). Diabetic Cardiomyopathy. Circulation research, 124(8), 1160–1162. https://doi.org/10.1161/CIRCRESAHA.118.314665.
2. Rubler S, Dlugash J, Yuceoglu YZ, Kumral T, Branwood AW, Grishman A. New type of cardiomyopathy associated with diabetic glomerulosclerosis. Amer J of Cardiology. 1972;30:595.
3. Kannel, W. B., Hjortland, M., & Castelli, W. P. (1974). Role of diabetes in congestive heart failure: the Framingham study. The American journal of cardiology, 34(1), 29–34. https://doi.org/10.1016/0002-9149(74)90089-7.
4. Jia G, Whaley-Connell A, Sowers JR. Diabetic cardiomyopathy: a hyperglycaemia- and insulin-resistance-induced heart disease. Diabetologia. 2018;61(1):21–28. doi:10.1007/s00125-017-4390-4.
5. Ma H, Li SY, Xu P et al (2009) Advanced glycation endproduct (AGE) accumulation and AGE receptor (RAGE) up-regulation contribute to the onset of diabetic cardiomyopathy. J Cell Mol Med 13:1751–1764.
6. Sokos GG, Nikolaidis LA, Mankad S, Elahi D, Shannon RP (2006) Glucagon-like peptide-1 infusion improves left ventricular ejection fraction and functional status in patients with chronic heart failure. J Card Fail 12:694–699.
7. Udell JA, Cavender MA, Bhatt DL, Chatterjee S, Farkouh ME, Scirica BM (2015) Glucose-lowering drugs or strategies and cardiovascular outcomes in patients with or at risk for type 2 diabetes: a meta-analysis of randomised controlled trials. Lancet Diabetes Endocrinol 3:356–366.
8. Eraky S M, Ramadan N M. Effects of omega-3 fatty acids and metformin combination on diabetic cardiomyopathy in rats through autophagic pathway[J]. The Journal of Nutritional Biochemistry, 2021:108798.
9. Zhen Y P, Zhao S B, Zhong M W, et al. The myocardial protective effects of puerarin on STZ-induced diabetic rats. [J]. Fen Zi XI Bao Sheng Wu Xue Bao, 2009, 42(2):137–144.

10. Xue J, Zhou N, Y Yang, et al. Puerarin-loaded ultrasound microbubble contrast agent used as sonodynamic therapy for diabetic cardiomyopathy rats[J]. Colloids and surfaces B: Biointerfaces, 2020, 190:110887.
11. Wang X, Zhao L. Calycosin ameliorates diabetes-induced cognitive impairments in rats by reducing oxidative stress via the PI3K/Akt/GSK-3β signaling pathway[J]. Biochemical and Biophysical Research Communications, 2016.
12. YY Zhang, Tan R Z, Zhang X Q, et al. Calycosin Ameliorates Diabetes-Induced Renal Inflammation via the NF-κB Pathway In Vitro and In Vivo[J]. Medical Science Monitor, 2019, 25:1671–1678.
13. Ru J, Li P, Wang J, Zhou W, Li B, Huang C, Li P, Guo Z, Tao W, Yang Y, Xu X, Li Y, Wang Y, Yang L. TCMSP: a database of systems pharmacology for drug discovery from herbal medicines. J Cheminform. 2014 Apr 16;6:13.
14. Piero J, JM Ramírez-Anguita, J Saüch-Pitarch, et al. The DisGeNET knowledge platform for disease genomics: 2019 update[J]. Nucleic Acids Research, 2019, 48(D1).
15. Shannon P, Markiel A, Ozier O, Baliga NS, Wang JT, Ramage D, Amin N, Schwikowski B, Ideker T. Cytoscape: a software environment for integrated models of biomolecular interaction networks. Genome Res. 2003;13(11):2498–504.
16. Damian S, Gable A L, Nastou K C, et al. The STRING database in 2021: customizable protein–protein networks, and functional characterization of user-uploaded gene/measurement sets[J]. Nucleic Acids Research, 2020(D1):D1.
17. Pinzi L, Rastelli G. Molecular Docking: Shifting Paradigms in Drug Discovery. Int J Mol Sci. 2019;20(18):4331.
18. Trott O, Olson AJ. AutoDock Vina: improving the speed and accuracy of docking with a new scoring function, efficient optimization, and multithreading. J Comput Chem. 2010 Jan 30;31(2):455–61.
19. Seeliger D, de Groot BL. Ligand docking and binding site analysis with PyMOL and Autodock/Vina. J Comput Aided Mol Des. 2010 May;24(5):417–22.
20. Collier TA, Piggot TJ, Allison JR. Molecular Dynamics Simulation of Proteins. Methods Mol Biol. 2020;2073:311–327.
21. Hess B, Kutzner C, David V, et al. GROMACS 4: Algorithms for Highly Efficient, Load-Balanced, and Scalable Molecular Simulation[J]. Journal of Chemical Theory & Computation, 2008, 4(3):435–447.
22. Cousins KR. Computer review of ChemDraw Ultra 12.0. J Am Chem Soc. 2011 Jun 1;133(21):8388.
23. Helen M. Berman, John Westbrook, Zukang Feng, Gary Gilliland, T. N. Bhat, Helge Weissig, Ilya N. Shindyalov, Philip E. Bourne, The Protein Data Bank, Nucleic Acids Research, Volume 28, Issue 1, 1 January 2000, Pages 235–242, https://doi.org/10.1093/nar/28.1.235.
24. Song, R., Zhao, X., Cao, R., Liang, Y., Zhang, D. Q., & Wang, R. (2021). Irisin improves insulin resistance by inhibiting autophagy through the PI3K/Akt pathway in H9c2 cells. Gene, 769, 145209. https://doi.org/10.1016/j.gene.2020.145209.
25. El-Sayed, N., Mostafa, Y. M., AboGresha, N. M., Ahmed, A., Mahmoud, I. Z., & El-Sayed, N. M. (2021). Dapagliflozin attenuates diabetic cardiomyopathy through erythropoietin up-regulation of AKT/JAK/MAPK pathways in streptozotocin-induced diabetic rats. Chemico-biological interactions, 347, 109617. https://doi.org/10.1016/j.cbi.2021.109617.
26. Zhao L, Wang Y, Liu J, et al. Protective Effects of Genistein and Puerarin against Chronic Alcohol-Induced Liver Injury in Mice via Antioxidant, Anti-inflammatory, and Anti-apoptotic Mechanisms. Journal of Agricultural and Food Chemistry. 2016 Sep;64(38):7291–7297. DOI: 10.1021/acs.jafc.6b02907.

27. Zhang, H., Zhang, L., Zhang, Q. et al. Puerarin: a novel antagonist to inward rectifier potassium channel (I K1). Mol Cell Biochem 352, 117–123 (2011). https://doi.org/10.1007/s11010-011-0746-0.
28. Zhen Y P, Zhao S B, Zhong M W, et al. The myocardial protective effects of puerarin on STZ-induced diabetic rats. [J]. Fen Zi XI Bao Sheng Wu Xue Bao, 2009, 42(2):137–144.
29. Zhang S, Qian W, Li S, et al. Effects of Huangqi Injection Combined with Puerarin Injection on KKAy Mice with Diabetic Cardiomyopathy on Endoplasmic Reticulum Stress[J]. World Chinese Medicine, 2017.

Figures

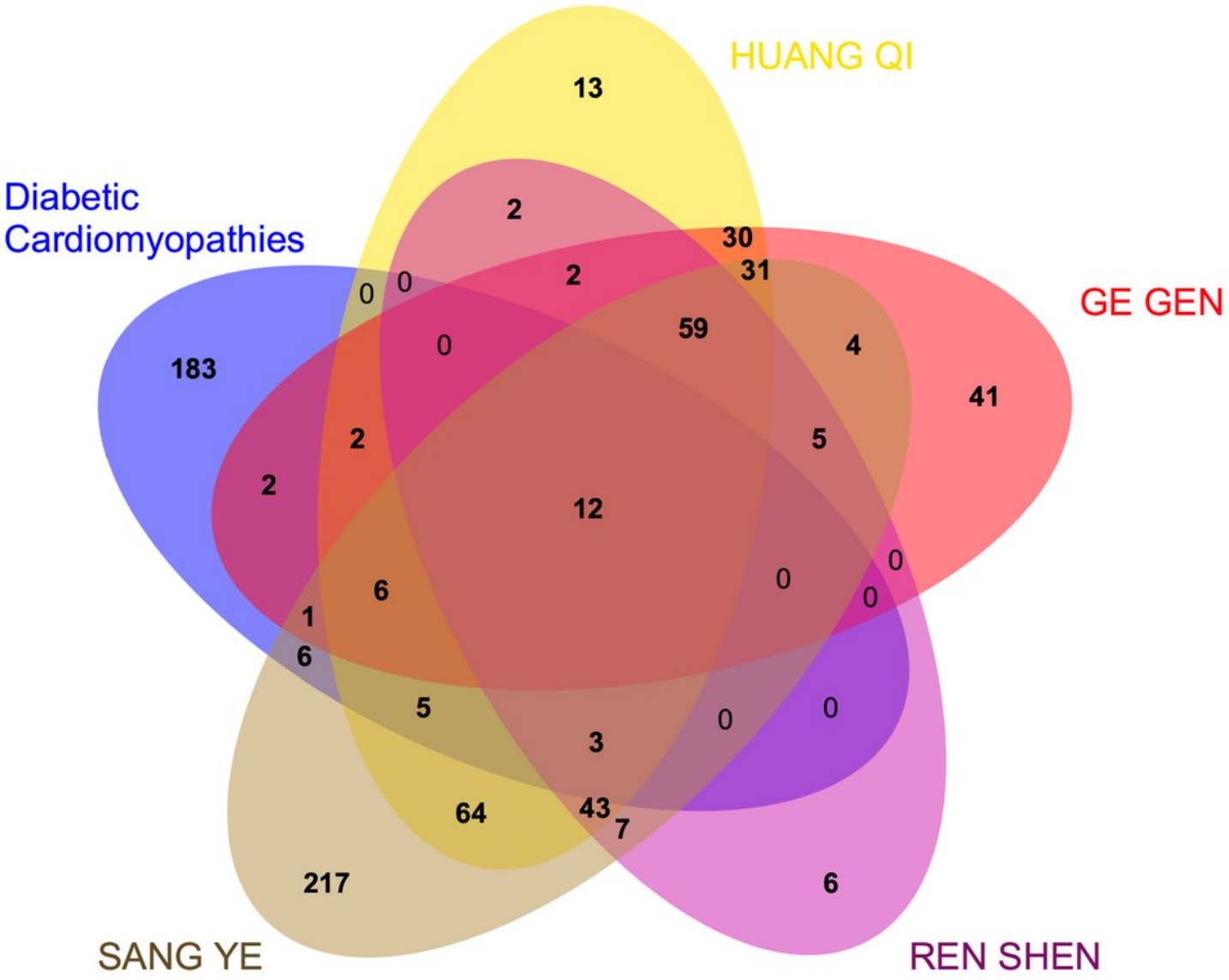

Figure 1

Intersection of active ingredient target and DC target

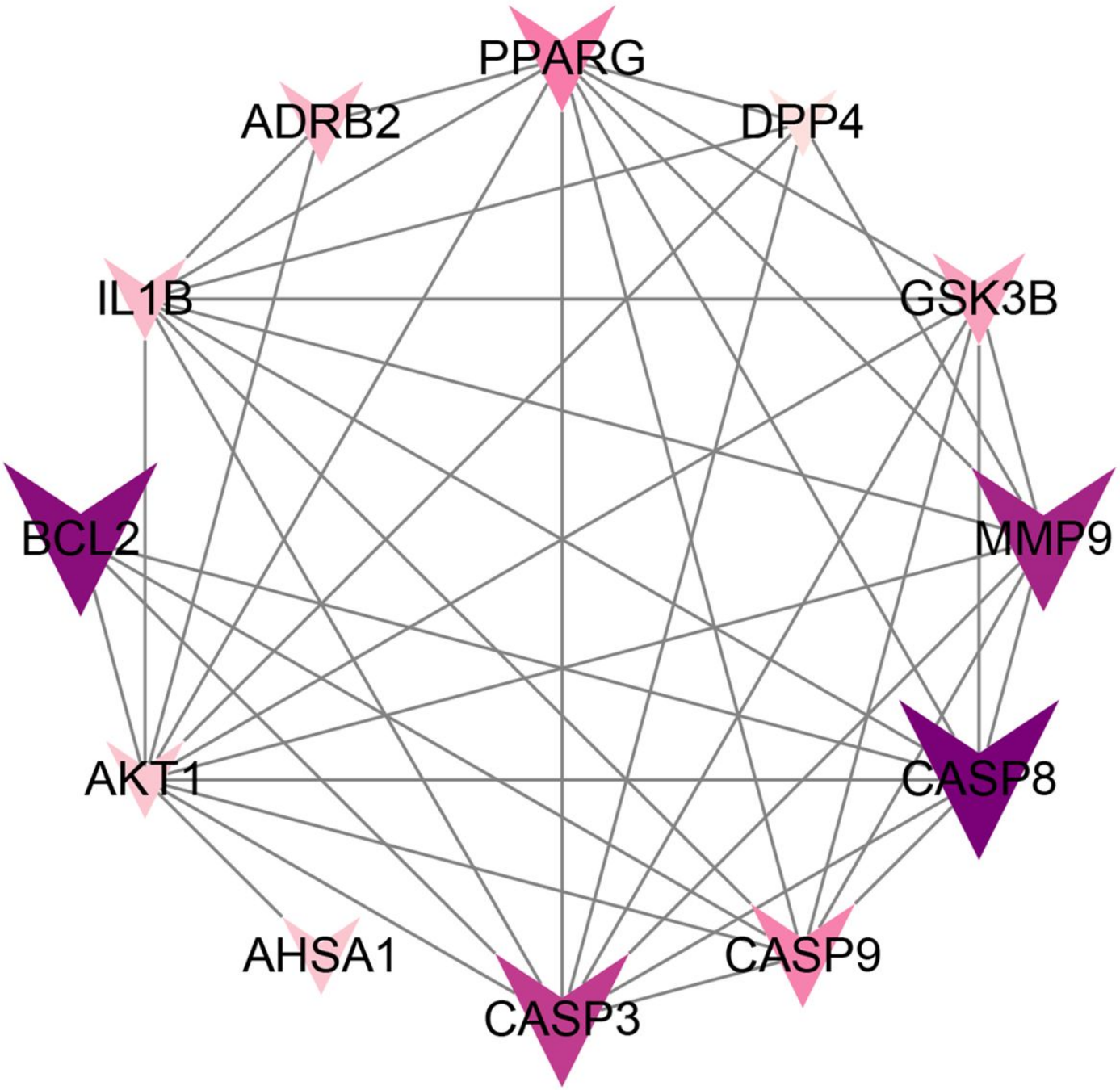

Figure 2

PPI network with 12 targets

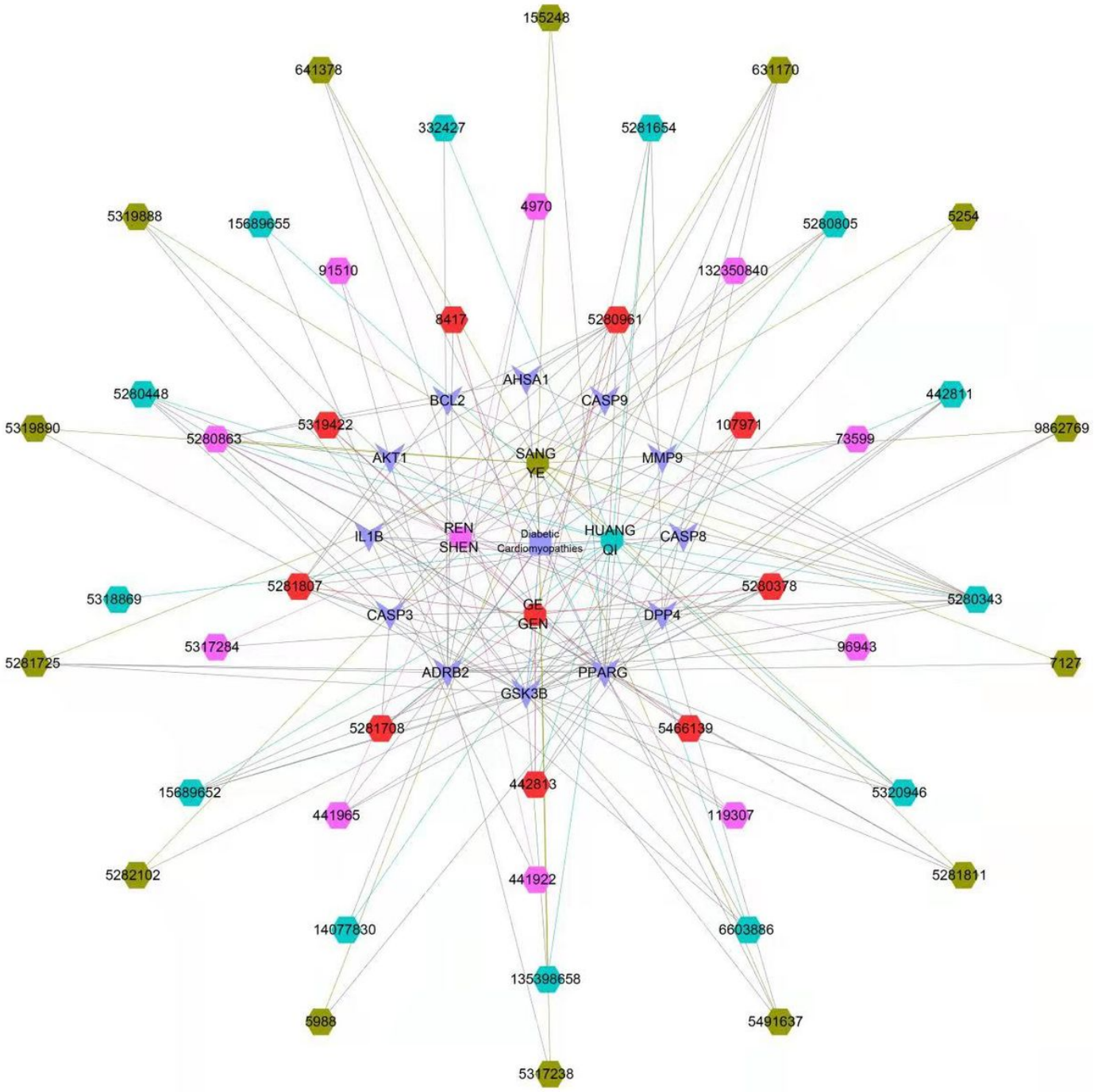

Figure 3

C-T-D network of active components and DC targets of four traditional Chinese medicines

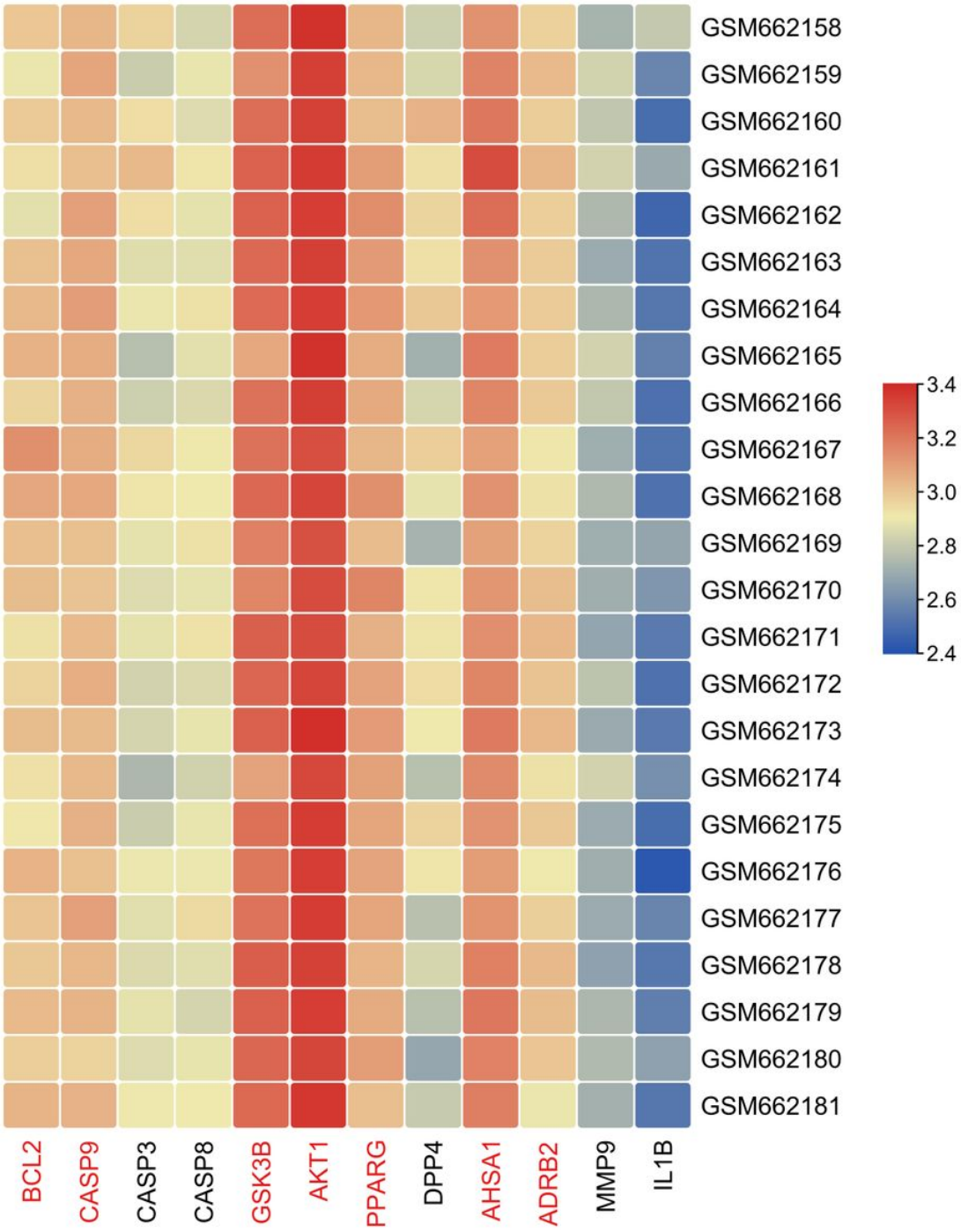

Figure 4

Expression of 12 targets in GSE26887 dataset

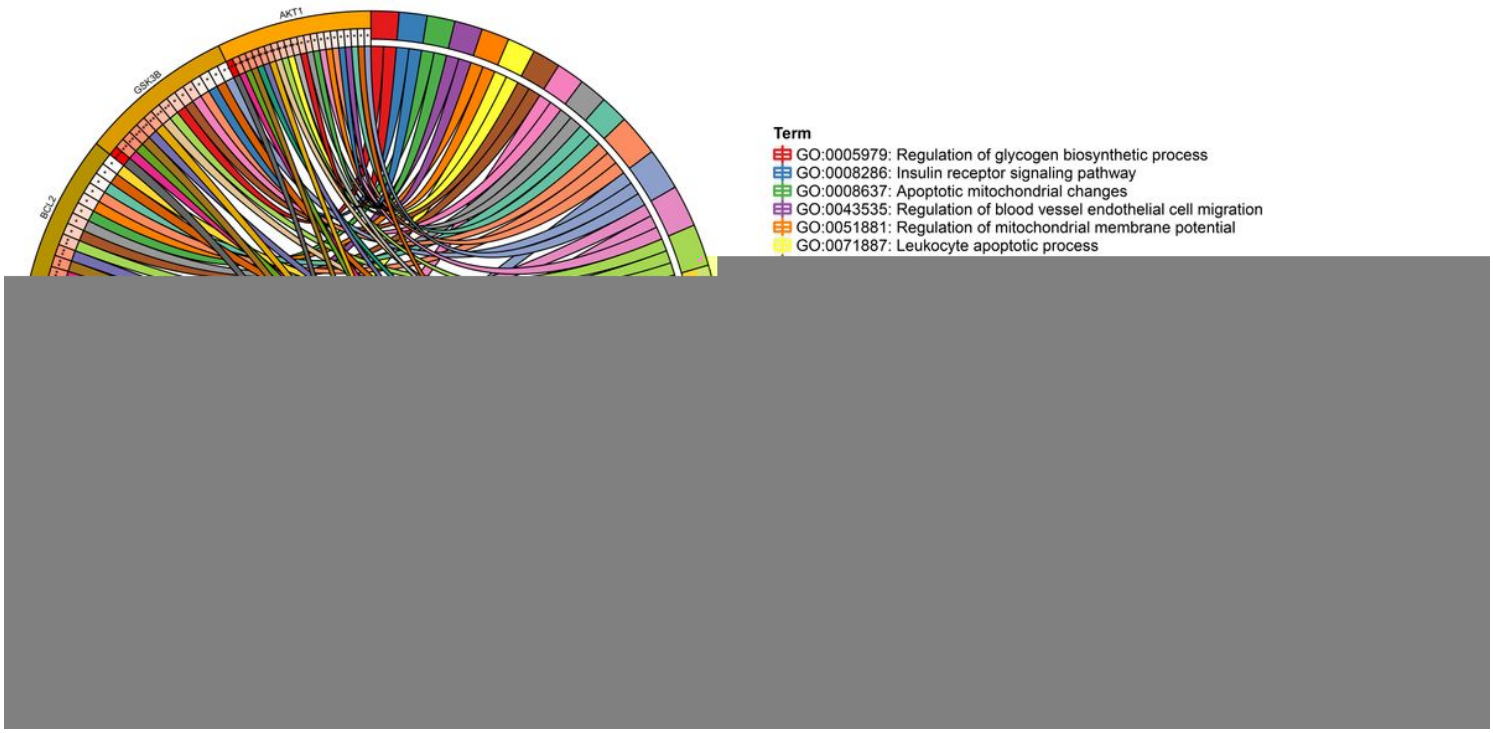

Figure 5

BP analysis of the final screened target

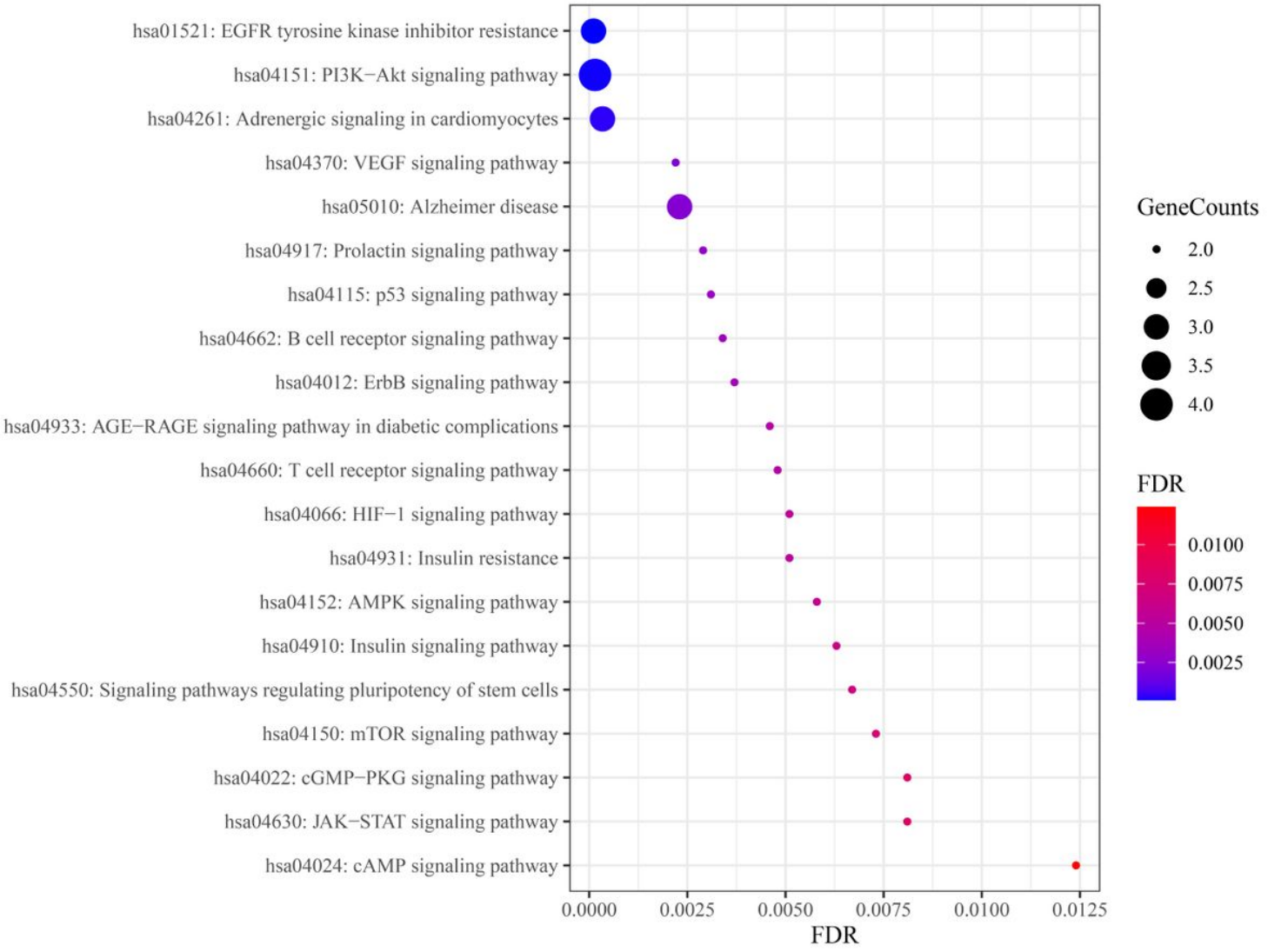

Figure 6

KEGG analysis of the final screened target

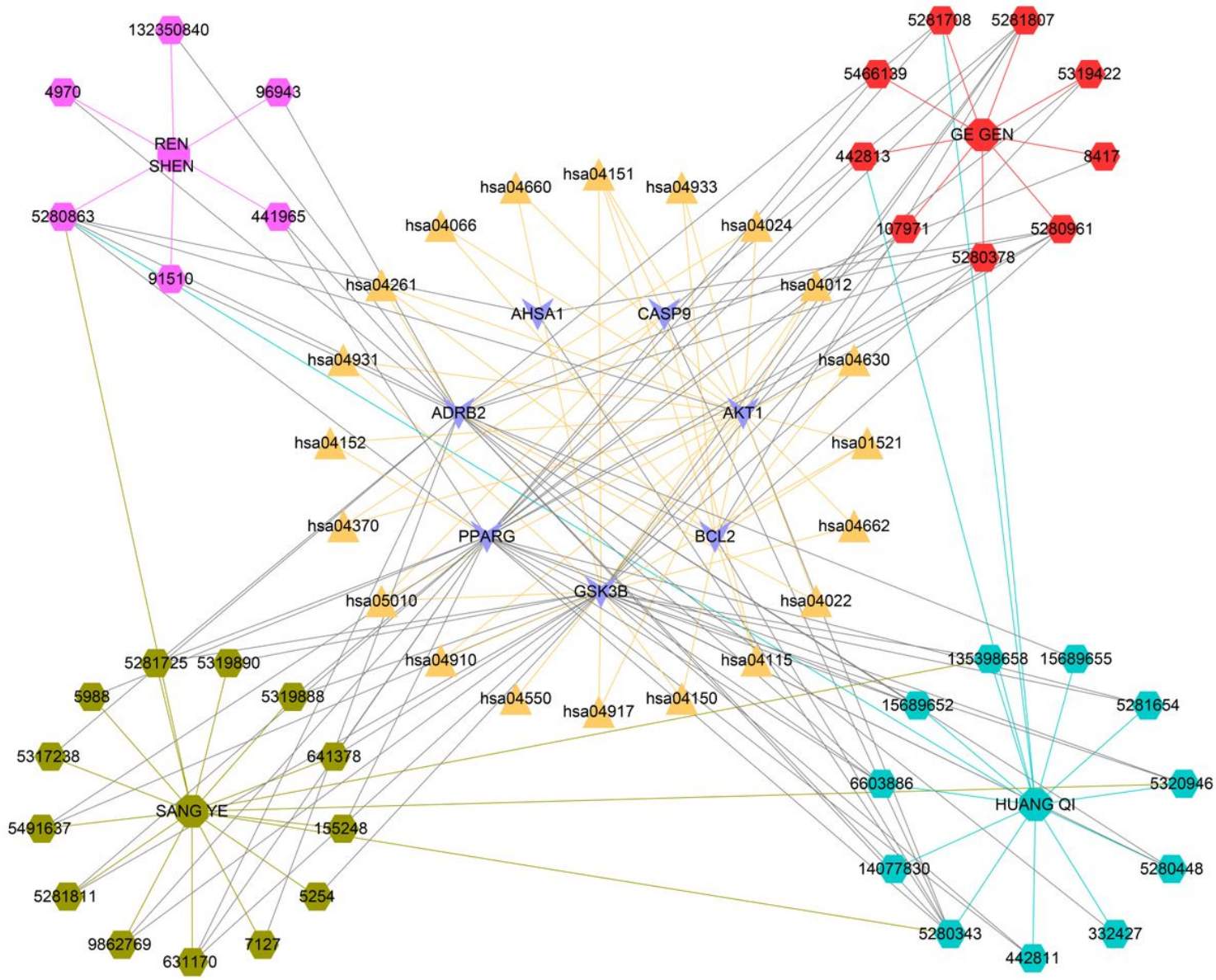

Figure 7

C-T-P network of components of 4 traditional Chinese medicines and DC targets

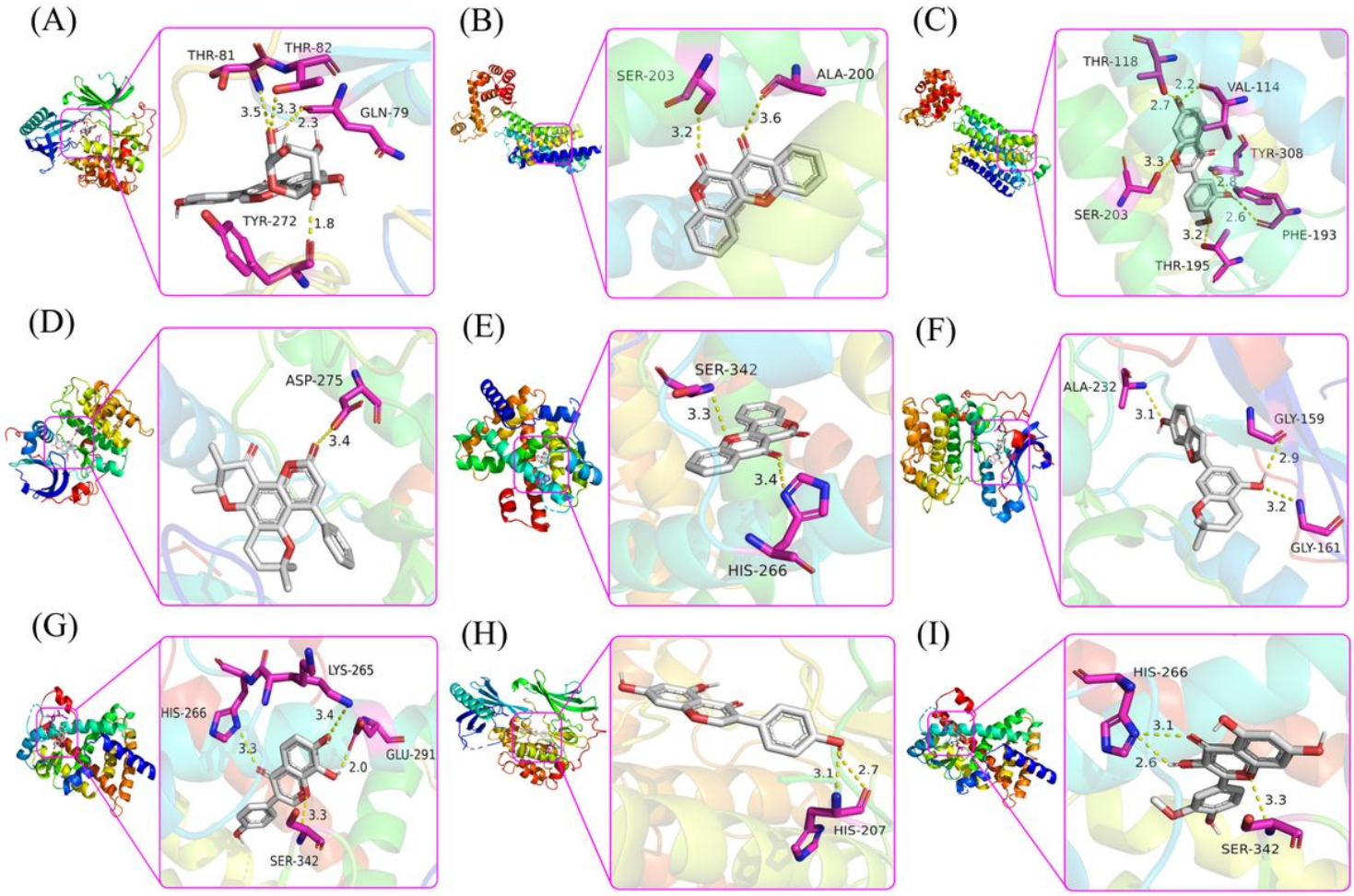

Figure 8

Molecular docking results of 8 components of traditional Chinese medicine and 4 proteins of DC, the connection represents a hydrogen bond. (a). Puerarin- AKT1 (b). Frutinone A- ADRB2 (c). Calycosin- ADRB2 (d). Inophyllum E-GSK3B (e). Frutinone A-PPARG (f). Moracin D- GSK3B (g). 8-Hydroxydaidzein-PPARG (h). Genistein- AKT1 (i). Isorhamnetin-PPARG

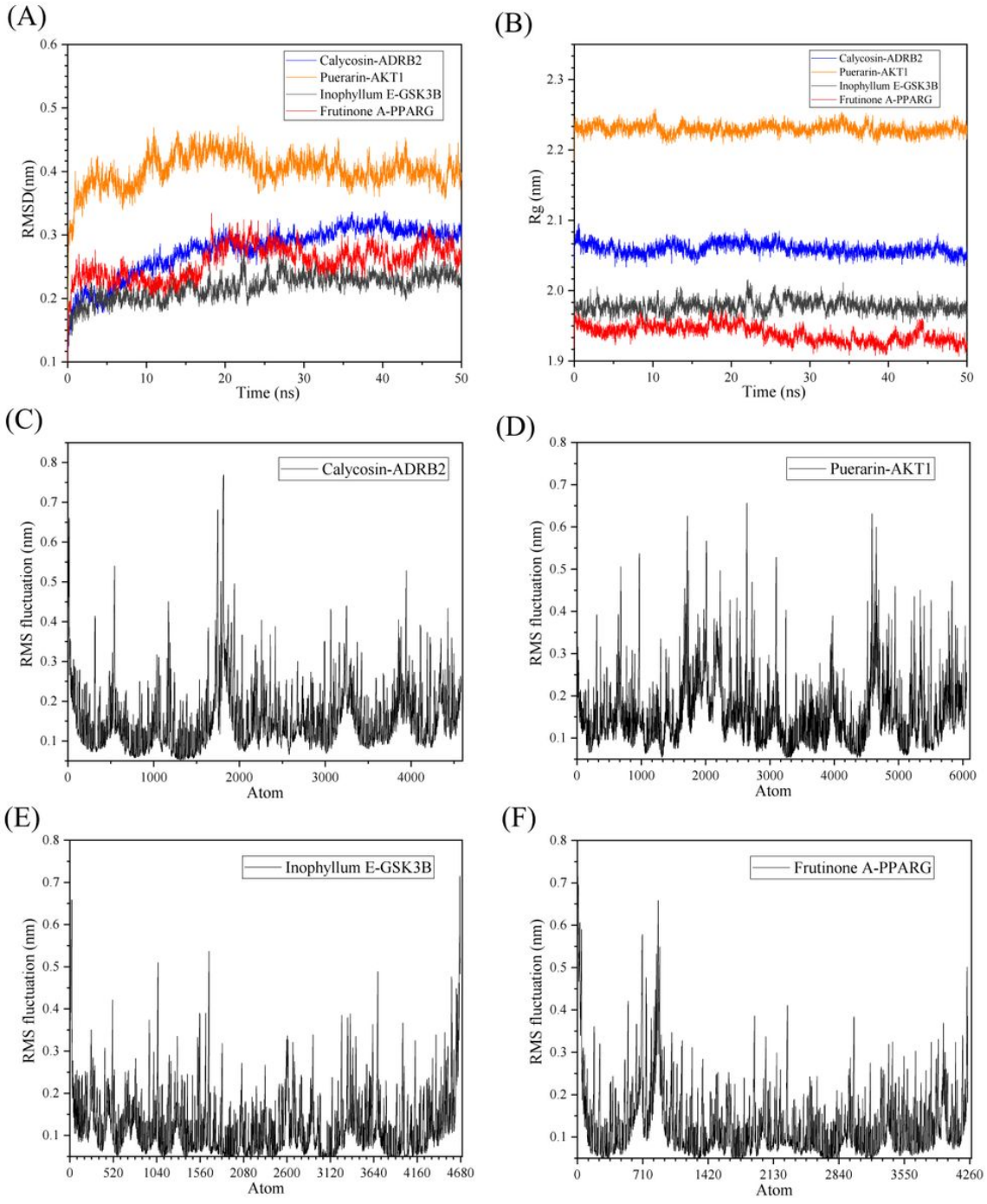

Figure 9

The results of MD simulation. (a). Root mean square deviation (RMSD) (b). Radius of gyration (Rg) (c, d, e, f). Root mean square fluctuation (RMSF)